Published OnlineFirst March 26, 2013; DOI: 10.1158/1078-0432.CCR-12-3726



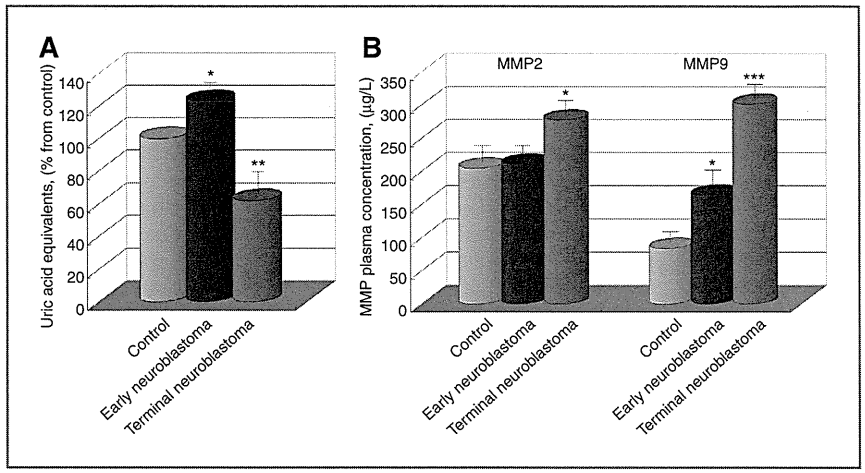


**Figure 7.** A, TAC of brain tissue in healthy and neuroblastoma-bearing mice. The data are the mean ± SD from 4 animals for each group. In the control group, TAC was considered 100%, which corresponded to 12 μmol/L uric acid equivalents per mg protein (~26 μmol/L copper reducing equivalents per mg protein). B, plasma levels of MMPs (MMP2 and MMP9) in healthy and neuroblastoma-bearing mice. The data are the mean ± SD from 4 animals for each group; *, $P < 0.05$; **, $P < 0.01$; ***, $P < 0.001$.

MRI signal in cancer-bearing mice injected with TEMPOL (partially water soluble, BBB-penetrating, and cell-penetrating), carbamoyl-PROXYL (water soluble, partially BBB-penetrating, and partially cell-penetrating), or carboxy-PROXYL (water soluble, BBB nonpenetrating, and cell nonpenetrating). The tumor was grafted in the right hind paw of C3H mice, and the left hind paw was used for comparison. The authors found that the intensity of the nitroxide-enhanced MRI/EPR signal in the noncancerous hind paw was significantly smaller than that in the cancer-bearing hind paw (22), which is similar to our observations (Fig. 3A). The authors do not provide data about the MRI/EPR signal decay in healthy mice. They have calculated that the rate of the MRI signal decay of TEMPOL and carbamoyl-PROXYL in cancerous tissue is more rapid than in noncancerous tissue of cancer-bearing mice. However, the ROI covers the central portion of the tumor (tumor core; ref. 22). It is very difficult for water-soluble and even partially hydrophobic substances to penetrate the tumor core, especially within a short time (within 15–20 minutes) and without a specific transport mechanism. In our studies, we observed a significant difference in the intensity and duration of the nitroxide-enhanced MRI signal between the tumor core and periphery in the terminal stage of cancer (data are not shown). In the tumor core, the signal enhancement was usually negligible even after the injection of cell-penetrating nitroxide (e.g., TEMPOL or SLENU). It is unclear whether the absence of a signal was a result of the rapid reduction of nitroxide or an inability to penetrate the tumor core. In this study, our ROI covers the entire cancer area, which minimizes the effect of different penetration and distribution of nitroxide in different parts of tumor (Figs. 2–5).

Most likely, for water-soluble nitroxides (such as carbamoyl-PROXYL and carboxy-PROXYL), the tumor is visualized predominantly on the basis of angiogenesis and the prolonged circulation of nitroxides in the bloodstream and/or prolonged retention in the EES of cancerous tissue. In this case, the MRI signal decay should be a result of nitroxide reduction in the bloodstream and/or EES and clearance from the organism through the kidneys. The same authors have shown that nitroxide-enhanced MRI signal appears first in kidney and after that in cancer area after injection of carboxy-PROXYL (23). Our previous report indicates that the penetration of nitroxide in cells and tissues is obligatory for MRI of the cancer based on the TRA (20).

Even when the BBB is disrupted (as in brain cancer), the water-soluble nitroxides are accumulated and retained in the EES despite penetrating the cells. This is a major contrast mechanism for the visualization of tumors using water-soluble gadolinium contrast agents.

In our study, we used SLENU, which is a strongly hydrophobic drug [octanol/PBS partition coefficient (log $P_{Oct/PBS}$) was 1.000 vs. 0.575 for TEMPOL, −0.158 for carbamoyl-PROXYL, and −2.000 for carboxy-PROXYL]. Nitrosoureas are well-known DNA-annealing agents, penetrating cellular and even nuclear membranes (35, 40). Thus, the dynamics of the nitroxide-enhanced MRI signal using SLENU (Figs. 2–5) could be attributed to its penetration into the cells and subsequent intracellular reduction/oxidation.

Recently, Davis and colleagues have reported that the dynamic of nitroxide-enhanced MRI is very heterogeneous in different tissues of the same cancer-bearing organism (24). We also established that the intensity, half-life, and duration of nitroxide enhancement were different in brain tissue, tissues around the brain, and muscle tissue of the hind paw (Figs. 3–5; refs. 21, 39). Moreover, different cancerous tissues (e.g., glioma and neuroblastoma) showed heterogeneous dynamic of nitroxide-enhanced MRI (Fig. 3A vs. 5B). Heterogeneity of the signal existed in the same cancerous tissue using different cell-penetrating nitroxide probes: SLENU or TEMPOL (Figs. 5 and 6). Therefore, the different rates of MRI signal decay could be a result of overlaping of several processes occuring simultaneously in tissues: different penetration rates, different reduction rates, different retention time, and different excretion rates of nitroxide from different tissues.

Published OnlineFirst March 26, 2013; DOI: 10.1158/1078-0432.CCR-12-3726



The different interpretations of the experimental data from the nitroxide-enhanced MRI studies that are published in the literature can be explained by several reasons: (i) the use of nitroxides with different cell-penetrating ability, place of retention, and excretion rate, (ii) the heterogeneity of the signal in different tissues (as a result of their different structure and metabolism), (iii) the heterogeneity of the signal in same tissue for different cell-penetrating nitroxide probes (as a result of their different pharmacokinetics), and (iv) the different analytic approaches (conclusions based on: rate of MRI signal decay, half-life of nitroxide-enhanced MRI signal, and intensity of nitroxide-enhanced MRI signal; refs. 19–24).

Each of the previous interpretations is correct, but none of them takes into account all factors that may affect the intensity and dynamics of nitroxide-enhanced MRI signal in living organism. To assess whether oxidation dominates over reduction in carcinogenesis or vice versa, it is necessary to compare the intensity and dynamics of nitroxide-enhanced MRI signal (rate of decay or half-life) in the same tissue between 2 animal species—healthy and cancer bearing. Only in this case, the penetration, retention, and excretion of nitroxide will occur at approximately same speed in the selected ROI, allowing us to ignore the impact of these factors on the dynamics of the signal. Because the cancerous tissue is completely different (structurally and metabolically) from noncancerous, presumably, the most indicative parameter for its redox activity is the duration of nitroxide-enhanced MRI signal. The presence of long-lived signal in the cancerous tissue, whereas in healthy tissues it is on baseline (Fig. 8), is an indicator for the presence of nitroxide in oxidized form, respectively, for the higher tissue-oxidative activity in cancer. The results with reduced TEMPOL support this assumption (Fig. 6). In the case of reduced TEMPOL, the nitroxide-enhanced MRI signal can appear only if noncontrast hydroxylamine is oxidized to contrast-enhancing nitroxide radical. The data showed that nitroxide enhancement appeared only in neuroblastoma-bearing brain in terminal stage, but not in healthy brain or neuroblastoma-bearing brain in early stage of cancer.

Our study also shows that the tissue redox balance is very sensitive to the progression of cancer and can be used as a diagnostic marker of carcinogenesis. In the early stage of cancer, the target tissue is characterized by a high-reducing activity, whereas it is characterized by a high-oxidative activity in the terminal stage. Carcinogenesis correlates with the redox potential of nontarget surrounding tissues and tissues distant from the tumor. In both stages of cancer development, the oxidative status of noncancerous tissues increases and they become susceptible to oxidative stress and damage.

What is the potential molecular mechanism(s) of these observations? Our hypothesis assumes that the inoculation of cancer cells in the brain can be considered an "inflammatory signal" (Fig. 9; refs. 41, 42). This inoculation leads to a local migration and an activation of a wide variety of immune cells in the target tissue, especially in the microenvironment of the primary tumor locus. This activation may trigger redox imbalance due to the "oxidative burst" of the immune cells and the production and release of ROS/RNS in the grafted area. In turn, this process will activate the antioxidant defense systems in the "inflamed" area as a compensatory mechanism to prevent oxidative stress in the microenvironment of the primary tumor locus (1, 41, 42). Our study shows that the TAC of the cancer-grafted brain slightly increased in the early stage of cancer development (Fig. 7A). Because the experiments were carried out on immunodeficient mice (Balb/c nude), the early phase was comparatively short (within 3–4 or 7–9 days for brain neuroblastoma or glioma, respectively). Shortly after inoculation, cell proliferation accelerated after overcoming the immune response, and the solid tumor grew.

The initial redox imbalance and subsequent signal transduction in the grafted area could be a critical regulator of cancer progression. ROS/RNS, produced by the immune cells in the primary tumor locus, could provoke signal transduction in 3 targets with equal probability: (i) the grafted cancer cells, (ii) the surrounding normal cells, and (iii) the surrounding extracellular matrix.

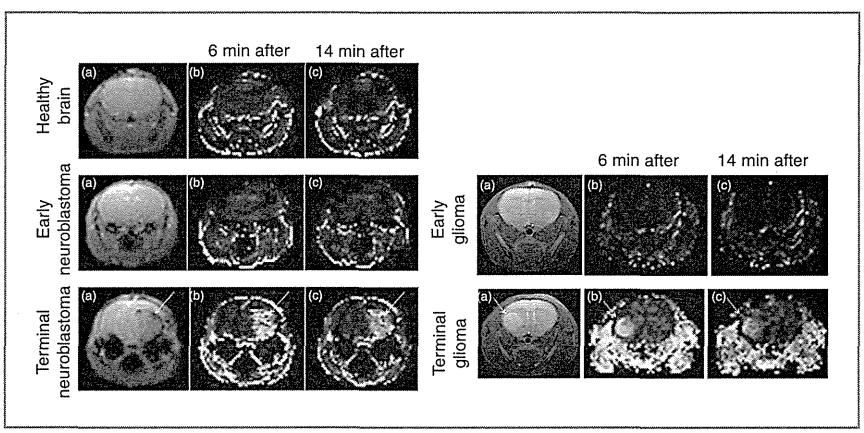


Figure 8. Typical nitroxide-enhanced MR images of healthy and cancer-bearing mice in the early or terminal stage of cancer (brain neuroblastoma or brain glioma). A, MR images of the brain with arrows indicating the tumor. B and C, extracted nitroxide-enhanced MRI signal obtained 6 and 14 minutes after injection of SLENU.

Published OnlineFirst March 26, 2013; DOI: 10.1158/1078-0432.CCR-12-3726



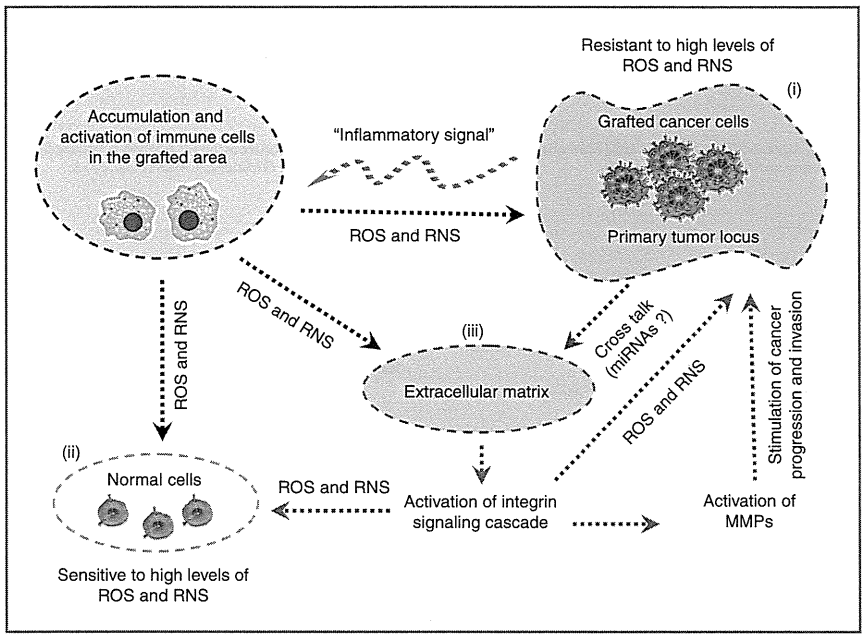


Figure 9. Molecular hypothesis. The inoculation of cancer cells in the brain can be considered an "inflammatory signal." The inoculation leads to a local migration and an activation of immune cells in the microenvironment of the primary tumor locus. ROS/RNS, produced by the activated immune cells in the grafted area, could provoke signal transduction in 3 targets with equal probability: (i) grafted cancer cells, (ii) surrounding normal cells, and (iii) the surrounding extracellular matrix. ROS/RNS and cross talk between cancer cells and the extracellular matrix activate the integrin signaling cascade. The oncogenic miRNAs, secreted by cancer cells into the environment, are considered a primary mediator of this process. The activation of integrins is linked to additional ROS/RNS production, leading to a vicious cycle. As a result, the tissue redox balance shifts toward oxidation. Cancer cells are adapted to high levels of ROS/RNS and survive. However, the normal surrounding cells and extracellular matrix are not adapted to this abnormal free radical attack and can undergo irreversible changes.

ROS/RNS have emerged as important mediators of signal transduction that are associated with the activation of the integrin pathway and modulation of integrin function through conformational changes (43). The cross talk between cancer cells and the extracellular matrix also activates integrin-related signal cascades. The oncogenic miRNAs, secreted by cancer cells into the environment, are considered a primary mediator of this process (44, 45). The activation of integrins is linked to additional ROS/RNS production by NADPH oxidases, lipoxygenases, mitochondria, etc., leading to a vicious cycle (46). As a result, the antioxidant defense system crashes with the progression of cancer and tissue redox balance shifts toward oxidation in the intermediate/terminal stage (Fig. 7A).

Integrin signaling also facilitates cell proliferation and migration, which is intimately linked to the degradation of the extracellular matrix, and activated MMPs are a prerequisite for cancer cell invasion (46). We established that the plasma level of MMP9 increases approximately 2 times even in the early stage of cancer development and approximately 3.5 times in the terminal stage (Fig. 7B). The plasma level of MMP2 also increases significantly in the terminal stage of cancer.

Cancer cells are adapted to the high levels of ROS/RNS and survive. However, the normal surrounding cells and extracellular matrix are not adapted to the abnormal free radical attack and can undergo irreversible changes. Our study also indicates that an antioxidant deficiency develops in tissues distant from the cancer locus of a cancer-bearing organism in the terminal stage. These normal tissues become highly sensitive to oxidative damage.

The data suggest that the cancerous and noncancerous tissues of a cancer-bearing organism are equally important therapeutic targets. Combining anticancer therapy with the protection of noncancerous tissues against oxidative stress may be essential for the survival and recovery of the organism.

## Disclosure of Potential Conflicts of Interest

No potential conflicts of interest were disclosed.

## Authors' Contributions

**Conception and design:** R. Bakalova, Z. Zhelev
**Development of methodology:** R. Bakalova, Z. Zhelev
**Acquisition of data (provided animals, acquired and managed patients, provided facilities, etc.):** R. Bakalova, I. Aoki
**Analysis and interpretation of data (e.g., statistical analysis, biostatistics, computational analysis):** R. Bakalova, Z. Zhelev, I. Aoki
**Writing, review, and/or revision of the manuscript:** R. Bakalova, Z. Zhelev, T. Saga
**Administrative, technical, or material support (i.e., reporting or organizing data, constructing databases):** I. Aoki
**Study supervision:** T. Saga

Published OnlineFirst March 26, 2013; DOI: 10.1158/1078-0432.CCR-12-3726



## Acknowledgments

The authors thank Ms. Sayaka Shibata and Mr. Nobuhiro Nitta (Molecular Imaging Center, National Institute of Radiological Sciences, Japan) for their participation in the MRI measurements.

## Grant Support

The study was partially supported by a grant-in-aid (Kakenhi) from the Ministry of Education, Science and Technology of Japan.

The costs of publication of this article were defrayed in part by the payment of page charges. This article must therefore be hereby marked *advertisement* in accordance with 18 U.S.C. Section 1734 solely to indicate this fact.

Received December 3, 2012; revised February 8, 2013; accepted March 2, 2013; published OnlineFirst March 26, 2013.

## References

1. Trachootham D, Alexandre J, Huang P. Targeting cancer cells by ROS-mediated mechanisms: a radical therapeutic approach? Nat Rev Drug Discov 2009;8:579–91.
2. Gius D, Spitz DR. Redox signaling in cancer biology. Antioxid Redox Signal 2006;8:1249–52.
3. Diaz B, Courtneidge SA. Redox signaling at invasive microdomains in cancer cells. Free Radic Biol Med 2012;52:247–56.
4. Irwin ME, Rivera-Del Valle N, Chandra J. Redox control of leukemia: from molecular mechanisms to therapeutic opportunities. Antioxid Redox Signal 2012;8:1349–83.
5. Ziech D, Franco R, Pappa A, Panayiotidis MI. Reactive oxygen species (ROS)-induced genetic and epigenetic alterations in human carcinogenesis. Mutat Res 2011;711:167–73.
6. Zienolddiny S, Ryberg D, Haugen A. Induction of microsatellite mutations by oxidative agents in human lung cancer cell lines. Carcinogenesis 2000;21:1521–6.
7. Trachootham D, Lu W, Ogasawara MA, Del Valle NR, Huang P. Redox regulation in cell survival. Antioxid Redox Signal 2008;10:1343–74.
8. Kroemer G, Pouyssegur J. Tumour cell metabolism: cancer's Achilles' heel. Cancer Cell 2008;13:472–82.
9. Kagan V, Bakalova R, Karakashev P. Lipid peroxidation in the tumour cells and tissues of tumour-bearing animals. In:Vigo-Pelfrey C, editor. Membrane lipid oxidation. Boca Raton (FL): CRC Press; 1992;Volume III:p. 191–208.
10. Gupta SC, Hevia D, Patchva S, Park B, Koh W, Aggrawal BB. Upsides and downsides of ROS for cancer: the roles of ROS in tumourogenesis, prevention, and therapy. Antioxid Redox Signal 2012;16:1295–322.
11. Mandal S, Lindgren AG, Srivastava AS, Clark AT, Banerjee U. Mitochondrial function controls proliferation and early differentiation potential of embryonic stem cells. Stem Cells 2011;29:486–95.
12. Fulda S, Galluzzi L, Kroemer G. Targeting mitochondria for cancer therapy. Nat Rev Drug Discov 2010;9:447–64.
13. Kroemer G. Mitochondria in cancer. Oncogene 2006;25:4630–2.
14. Sanchez-Aragó M, Formentini L, Cuezva M. Mitochondria-mediated energy adaptation in cancer: the H(+)-ATP synthase-geared switch of metabolism in human tumors. Antioxid Redox Signal. 2012 Sep 24. [Epub ahead of print].
15. Chan EC, Jiang F, Peshavariya HM, Dusting GJ. Regulation of cell proliferation by NAHDH oxidase-mediated signaling: potential role in tissue repair, regenerative medicine and tissue engineering. Pharmacol Ther 2009;122:97–108.
16. Hayes P, Knaus UG. Balancing reactive oxygen species in the epigenome: NADPH oxidases as target and perpetrator. Antioxid Redox Signal. 2012 Nov 5. [Epub ahead of print].
17. Chaiswing L, Zhong W, Liang Y, Jones DP, Oberley TD. Regulation of prostate cancer cell invasion my modulating of extra- and intracellular redox balance. Free Radic Biol Med 2012;52:452–61.
18. Hamanaka RB, Chandel BS. Mitochondrial reactive oxygen species regulate hypoxic signaling. Curr Opin Cell Biol 2009;21:894–9.
19. Zhelev Z, Bakalova R, Aoki I, Gadjeva V, Kanno I. Imaging of cancer by redox-mediated mechanism: a radical diagnostic approach. Mol BioSyst 2010;6:2386–8.
20. Zhelev Z, Gadjeva V, Aoki I, Bakalova R, Saga T. Cell-penetrating nitroxides as molecular sensors for imaging of cancer *in vivo*, based on tissue redox activity. Mol BioSyst 2012;8:2733–40.
21. Zhelev Z, Aoki I, Gadjeva V, Nikolova B, Bakalova R, Saga T. Tissue redox activity as a sensing platform for imaging of cancer based on nitroxide redox cycle. Eur J Cancer. 2012 Dec 19. [Epub ahead of print].
22. Matsumoto K, Hyodo F, Matsumoto A, Koretsky AP, Sowers AL, Mitchell JB, et al. High-resolution mapping of tumor redox status by MRI using nitroxides as redox-sensitive contrast agents. Clin Cancer Res 2006;12:2355–62.
23. Hyodo F, Matsumoto K, Matsumoto A, Mitchell JB, Krishna MC. Probing the intracellular redox status of tumors with magnetic resonance imaging and redox-sensitive contrast agents. Cancer Res 2006;66:9921–8.
24. Davis RM, Matsumoto S, Brnardo M, Sowers A, Matsumoto K, Krishna MC, et al. Magnetic resonance imaging of organic contrast agents in mice: capturing the whole-body redox landscape. Free Rad Biol Med 2011;50:459–68.
25. Fuchs J, Groth N, Herrling T, Zimmer G. Electron paramagnetic resonance studies on nitroxide radical 2,2,5,5-tetramethyl-4-piperidin-1-oxyl (TEMPO) redox reactions in human skin. Free Radic Biol Med 1997;22:967–76.
26. Batinic-Haberle I, Reboucas JS, Spasijevic I. Superoxide dismutase mimetics: chemistry, pharmacology, and therapeutic potential. Antioxid Redox Signal 2010;13:877–918.
27. Mehlhorn RJ. Ascorbate- and dehydroascorbic acid-mediated reduction of free radicals in the human erythrocytes. J Biol Chem 1991;266:2724–31.
28. Bobko AA, Kirilyuk IA, Grigor'ev IA, Zweier JL, Khramtsov VV. Reversible reduction of nitroxides to hydroxylamines: the roles for ascorbate and glutathione. Free Radic Biol Med 2007;42:404–12.
29. Matsumoto A, Matsumoto K, Matsumoto S, Hyodo F, Sowers AL, Koscielniak JW, et al. Intracellular hypoxia of tumor tissue estimated by noninvasive EPR oximetry technique using paramagnetic probes. Biol Pharm Bull 2011;34:142–5.
30. Ui I, Okajo A, Endo K, Utsumi H, Matsumoto K. Effect of hydrogen peroxide in redox status estimation using nitroxyl spin probe. Free Radic Biol Med 2004;37:2012–7.
31. Soule BP, Hyodo F, Matsumoto K, Simone NL, Cook JA, Krishna MC, et al. Therapeutic and clinical applications of nitroxide compounds. Antioxid Redox Signal 2007;9:1731–42.
32. Hyodo F, Soule BP, Matsumoto K, Matsumoto S, Cook JA, Hyodo E, et al. Assessment of tissue redox status using metabolic responsive contrast agents and magnetic resonance imaging. J Pharm Pharmacol 2008;60:1049–60.
33. Hyodo F, Murugesan R, Matsumoto K, Hyodo E, Subramanian S, Mitchell JB, et al. Monitoring redox-sensitive paramagnetic contrast agent by EPRI, OMRI and MRI. J Magn Reson 2008;190:105–12.
34. Rosen GM, Cohen MC, Britigan BE, Pou S. Application of spin traps to biological systems. Free Radic Res Commun 1990;9:187–95.
35. Zhelev Z, Matsumoto K, Gadjeva V, Bakalova R, Aoki I, Zheleva A, et al. EPR signal reduction kinetic of several nitroxyl derivatives in blood *in vitro* and *in vivo*. Gen Physiol Biophys 2009;28:356–62.
36. Okajo A, Matsumoto K, Mitchell JB, Krishna MC, Endo K. Competition of nitroxyl contrast agents as an *in vivo* tissue redox probe: comparison of pharmacokinetics by the bile flow monitoring (BFM) and blood circulating monitoring (BCM) methods using X-band EPR and simulation of decay profiles. Magn Reson Med 2006;56:422–31.
37. Hyodo F, Chuang KH, Goloshevsky AG, Sulima A, Griffiths GL, Mitchell JB, et al. Brain redox imaging using blood-brain barrier-permeable nitroxide MRI contrast agent. J Cereb Blood Flow Metab 2008;28:1165–74.

Published OnlineFirst March 26, 2013; DOI: 10.1158/1078-0432.CCR-12-3726




38. Gadjeva V. Structure-based design of nitrosoureas containing tyrosine derivatives as potential antimelanoma agents. Eur J Med Chem 2002;37:295–7.
39. Zhelev Z, Bakalova R, Aoki I, Matsumoto K, Gadjeva V, Anzai K, et al. Nitroxyl radicals for labeling of conventional therapeutics and noninvasive magnetic resonance imaging of their permeability for blood-brain barrier: relationship between structure, blood clearance, and MRI signal dynamic in the brain. Mol Pharm 2009;6:504–12.
40. Lage H, Dietel M. Involvement of the DNA mismatch repair system in antineoplastic drug resistance. J Cancer Res Clin Oncol 1999;125:156–65.
41. Kundu JK, Surh Y-J. Emerging avenues linking inflammation and cancer. Free Radic Biol Med 2012;52:2013–37.
42. Paez D, Labonte MJ, Bohanes P, Zhang W, Benhanim L, Ning Y, et al. Cancer dormancy: a model of early dissemination and late cancer recurrence. Clin Cancer Res 2011;18:645–53.
43. Gregg D, de Carvalho DD, Kavacic H. Integrins and coagulation: a role for ROS/redox signaling? Antioxid Redox Signal 2004;6:757–64.
44. Rutnam ZJ, Wight TN, Yang BB. miRNAs regulate expression and function of extracellular matrix molecules. Matrix Biol. 2012 Nov 15. [Epub ahead of print].
45. Dalmay T, Edwards DR. MicroRNAs and the hallmarks of cancer. Oncogene 2006;25:6170–5.
46. Svineng G, Ravuri C, Rikardsen O, Huseby NE, Winberg JO. The role of reactive oxygen species in integrin and matrix metalloproteinase expression and function. Connect Tissue Res 2008;49:197–202.

# 平成２５年度第三次対がん総合戦略研究事業

研究課題：　悪性中皮腫に対する単剤多機能抗がん治療の開発
課題番号：　H24-3次がん-一般-005
研究代表者：横浜市立大学大学院医学研究科　循環制御医学
　　：石川義弘

１．本年度の研究成果

石綿による健康被害（石綿症）は１９００年代から知られていたが、我が国で法規制が開始されたのは７５年以降であり、本格的な労働者に対する規制は２００５年以降である。悪性中皮腫は胸膜中皮由来の腫瘍であり石綿暴露との関連が強いが、発症まで２０－５０年を要する。このため今後十数年間は我が国の患者数の増加が予測される。発見時には外科的根治術が困難であり、放射線や化学治療にも腫瘍としての抵抗性が強く、極めて低い治療成績である。化学療法としてシスプラチン、或はペメトレキセド併用療法が基本だが、薬剤の投与量は、副作用の発現によって制限を受ける。また一部の先進医療機関では、温熱療法が併用されているが、症状緩和に有効ではあるが、積極的な治療法ではない。

悪性腫瘍に対する温熱療法の歴史は１９世紀と古いが、現代的な治療に応用されたのは６０年代からである。細胞実験ではがん細胞は42.5度以上になると細胞死を起こしやすくなる。そこで電磁波を用いてがん組織全体を暖め、化学療法の効果の増強を狙ったマイルド温熱による全身温熱療法が採用されている。これはあくまでも化学療法の補助療法であり、副作用は少ないが治療効果も高度ではない。近年欧米で実用化された方法は、局所温熱による積極的な治療法である。鉄などの磁性微粒子を腫瘍組織に直接注入し、交流磁場印加によって発熱させ、がん細胞を殺傷する仕組みである。然るに使用されるのは抗がん作用を持たない鉄粒子を発熱体として使用するのみである。抗がん剤を腫瘍組織に同時注入すると、磁性粒子による発熱のため抗がん剤が変性してしまうからである。温熱治療と化学療法が同時施行できれば、治療効果は画期的に増強することが期待できる。

我々の研究では、これまで治療困難とされる悪性中皮腫に対して、化学療法と温熱療法の「同時施行」を検討した。このためには既存の抗がん剤や鉄粒子ではなく、新規磁性抗がん剤（ＥＩ２３６）を用いる。シスプラチン様の強い抗がん作用を有するだけでなく、交流磁場印加によって強い発熱作用を持つ。このため抗がん作用が熱変性することがなく、反復性の交流磁場印加・温熱治療が可能であることが分かった。中皮腫細胞が温熱感受性をもち、本抗がん剤を中皮腫局所に磁場誘導することができ、さらに交流磁場印加で発熱できれば、温熱・化学療法の同時施行ができるようになり、悪性中皮腫に対して有効性を高めた治療法として開発ができると考えられた。とりわけ欧米で先鞭をつけられた鉄微粒子による局所温熱療法に対して、それを凌駕する画期的ながん治療法を日本から世界に向けて発信することができると考えられる。

昨年度からの継続実験において、ヒト由来の悪性中皮腫細胞における温熱感受性を検討した。ヒト由来の細胞株は複数種確立されており、これらの異なった株種に対して同様の検討を行った。温熱感受性については株間でも類似し、４２度で効果を示すが、４３度程度にまで上昇させても温熱感受性を示すことが分かった。温熱感受性は狭い温度域でのみ有効なわけではなく、他の癌細胞腫と同様に比較的ひろい温度枠を設定することができることが分かった。またこの温度枠において、EI236との併用によりいずれも抗がん活性が亢進することが確認された。昨年度の実験結果から、EI236が10μM前後において温熱刺激なしで50%程度の生存性が、温熱存在下においては最大30%以下に低下し、さらに薬剤濃度を高めると、細胞生存性は容量依存性に低下するが、温熱による細胞殺傷増強作用は低下することがわかっている。本年度の結果と合わせて、温熱効果が最大限に発揮できる抗がん剤濃度を検討し、最低量の治療濃度で治療を行うことが、効果的な治療法に結びつくことが確認された。

EI236の発熱特性の制御には、薬剤濃度以外に、交流磁場発生装置の性能が重要な役割を果たすことが分かった。これは出力だけの問題ではなく、使用する周波数と電力によって規定されることが分かった。さらに周波数特性によって、深部到達度を調節できることがわかり、これは悪性中皮腫の治療にあたって、皮膚からの深度により、周波数特性を変化させることによって発熱効果を最適化できることが分かった。我々の試作機であるYOKI-1500は単一条件でEI236に高い発熱を起こさせるが、さらに、周波数特性変換機能を持たせた機械によって、発熱や深部を調節できることがわかった。悪性中皮腫においても胸腔内での発現部位や深度が異なることから同機能は重要であると考えられた。

昨年度の研究結果から、マウス生体レベルで胸腔内において集積させることが可能であることがわかったが、これには大型棒磁石を体表面から当てるか、特殊小型磁石を胸腔皮下に埋め込むことが必要であった。然るに、ヒト応用にあたっては実用的ではない。そこでピップエレキ盤様の小型磁石を衣料ベストに縫込み、動物に磁石入りベストを着用させることで胸腔部分への集積が可能であるかを検討した。市販の小型磁石を縫い込んだベストを作成し、EI236を胸腔内に注入した後に、磁石部分がマウス胸壁にあたるようにベストを装着させ、マウスを3日間自由行動とさせた。マウス胸壁を取り出し、EI236を特殊染色したところ、ベスト磁石装着部に一致して強い集積反応が見られた。このことは磁石ベスト装着によってEI236を局所に誘導できたことを示す。同様の実験を腹腔においても行ったところ、強い集積を得ることができた。ヒトにおいてはさらに強力な小型磁石が複数必要になると考えられるが、極めて低い侵襲性で、体表面から磁場誘導を胸壁に対してかけることが可能と考えられる。

EI236による治療効果の評価においては、動物モデルでは胸壁を摘出せねばならず、時間経過による治療効果を実験的に評価することが困難である。そこで生体レベルで中皮腫組織の増減を観察できるよう、MRIによる画像診断の手法を開発した。先行研究から、マウスに中皮腫を移植して、マウス悪性中皮腫モデルを作成することが可能であることが分か

っている。このモデルにおいて、MRIの撮影条件を検討することにより、中皮腫のMRIによる非侵襲的な形態観察が可能であることがわかった。さらに確立された悪性中皮腫マウスモデルにおいて、EI236を投与し、体表面から磁場誘導をかけた。このMRI画像モデルにおいても、EI236がMRIシグナルとして検出できることが分かった。このことは、悪性中皮腫患者にEI236を投与した場合に、薬剤が腫瘍部位にどの程度到達したかを判定する可能性を強く示すものである。さらに磁場誘導をかけた後に、腫瘍部位への集積の程度を非侵襲的に定量する可能性を示す。

さらに我々は、理研のSpring8を用いたEI236の結晶構造解析結果から、数十年前に開発され、現在世界で幅広く使用されている既存の抗がん剤を磁性化した。この磁性抗がん剤は、抗がん作用として基本的な薬理学的な特徴を維持しながら、磁場誘導によって局所に誘導させることが可能であることが分かった。さらにMRIにおいて画像測定が可能であることも分かった。

以上の平成２５年度の実験結果から、１）多数のヒト悪性中皮腫細胞株はEI236に対して高い薬剤感受性と温熱感受性を示すこと、２）交流磁場印加装置の最適化により、組織における磁場印加の条件が検討され、この条件下でヒトへの応用性が高まること、3）マウス生体レベルで非侵襲的に磁石によるEI236の集積方法が確立されたこと、4）EI236の治療効果を経時的に観察できるマウス悪性中皮腫モデルが確立され、マウス生体において磁場誘導をMRIで評価することができること、５）既存の抗がん剤の磁性化ができること、が判明した。これらの検討結果は、EI２３６を用いた悪性中皮腫の新規治療法の開発が極めて有望なものになる可能性が示された。今後はさらにヒト臨床応用を目標に、研究を発展させていきたい。

２．研究成果の意義および今後の発展性

抗がん剤に限らず一般の医薬品化合物は、磁場誘導に対して十分な磁性を持たないとされる。しかしコバルトや鉄（磁性）粒子は磁石に付く。そこで磁性鉄粒子を利用して温熱療法や磁場誘導を行う研究が６０年代より進められてきた。一般的な手法は、鉄粒子と抗がん剤を混ぜ合わせてリポソームに包み、全体を磁石で誘導する。しかしながら、合成段階において抗がん剤と鉄粒子の両方が確実にリポソームに包埋されているのか、あるいは比率が１：１で常に包埋されるかなどの問題があった。さらには空リポソームの存在や、熱やｐＨによってリポソームが変性分解するため不安定、経口投与が困難などの諸問題がある。とくに温熱療法との併用においては、熱によってリポソームが分解してしまうため、施行が困難である。

造船業おける船舶の金属材料の開発には磁性の制御が必須であり、IHI（株）の基盤技術研究所では高度な磁性評価の技術を有する。エレクトロニクス分野ではこの技術を有機ダイオードなどの開発に応用している。我々はそれを医薬品化合物に応用し、新規磁性抗がん剤化合物（EI236）が開発された。本抗がん剤はシスプラチン類似薬であり、ＩＨＩ（株）

（旧石川島播磨重工業）の造船業におけるエンジンの金属材料開発技術を、医薬品化合物開発に応用して開発された。横浜市立大学先端医科学研究センターの援助を受けて実用化の検討段階に移行しており、多数の国内・国際特許によっても支持された独占的な先進技術である。本研究は学際的な共同研究者よりなる。本研究で対をなす温熱・磁場装置に関しては、横浜国大をはじめとする工学研究者（竹村泰司教授）どの協力を得て試作品YOKI-1500による検討を繰り返してきた。本年度の研究成果から、本試作品をどのように改良していくかの道筋が示された。また放射医学総合研究所のＭＲＩ分子イメージ専門家（青木伊知男チームリーダー）による悪性中皮腫の検討においては、生体レベルで EI236を可視化することに成功している。これは画像化可能な抗がん剤として重要な役割を果たすことができると考えられる。

過去８年間に及ぶ先行研究において、磁性を有する抗がん剤化合物が複数同定された。本年度の研究成果から、新規磁性抗がん剤を見つけるだけでなく、既存の抗がん剤に対して磁性特性を付与することが可能であることが示された。同様の手法を用いることにより、抗がん剤のみならず、他分野の医薬品化合物を磁性化する可能性が生まれた。これは患部への集積が望ましいと考えられる医薬品すべてに磁性化特性を与えることにより、磁場誘導により局所化できる可能性をしめす。さらに MRI による生体レベルでの画像化が可能であることから、生体内に投与した後にどのような分布を示すのかを画像診断することが可能になると期待される。本技術は純国産技術であり、学際技術であるとともに、造船業の技術を医学に転用した、産学連携の象徴的な技術開発であると考えられ、今後の我が国の産業振興にも貢献できると考えている。

今後数十年間にわたって患者が増大すると考えられる悪性中皮腫の根治的治療法は胸膜肺全的術であるが、診断時にはすでに広範に進展していることが多く、外科手術の適応とならないことが多い。外科治療は侵襲的であり、死亡率は高齢者ほど高いため、好発する高齢者でむしろ慎重な対応が必要である（日本肺癌学会ガイドライン）。手術不適応例に対しては放射線療法や化学療法がおこなわれるが、抗がん剤による治療は７５歳以上の高齢者には推奨されていない。そのため今後増加が予測されている高齢者に対する化学療法としては、国民的な解決課題と考えられる。高齢者は抗がん剤に対して副作用の発現が高いため、少量で有効な抗がん剤が必要である。また肝腎機能の低下により、副作用の発現予想が困難である。そこで体表面積から類推するだけでなく、テイラーメード的な投与量の決定が必要である。さらに症状緩和だけを目的とした温熱療法ではなく、治療効果の増強が期待できるハイパーサーミア療法の確立が必要である。磁性抗がん剤はそのいずれにも対応できる抗がん治療が可能であり、とりわけ「胸膜は胸壁から浅い」ため、磁場による誘導（ドラッグデリバリー）が可能となり、磁性抗がん剤の適応である。今回の検討結果から、その実用化への可能性が強く示された。

本研究により、磁性抗がん剤による高齢者に向けた安心・安全な悪性中皮腫の抗がん治療を開発することが、本申請の最大の目標であり社会貢献である。

３．倫理面への配慮

本研究は、厚生労働省の所管する実施機関における動物実験等の実施に関する基本指針及び横浜市立大学医学部で定めた倫理規定等を遵守して行う。動物を用いた実験は、動物実験の講習を修了し、充分な知識と経験を有するものだけに従事させる。産学連携、他施設共同、臨床試験、薬事申請に当たっては、関係者および関係施設における利益相反を中心に守秘義務など各種コンプライアンスを十分に順守して行う。また生物統計においては、動物愛護の観点から、必要とされる動物数などを最小限にとどめるため、本学臨床試験センターの指導下で生物統計の専門家の指導を受けつつ行う。

４．発表論文など

1. Okamoto Y, Hirota M, Monden Y, Murata S, Koyama C, Mitsudo K, Iwai T, Ishikawa Y, and Tohnai I:Hight-dose zoledronic acid narrows the periodontal space in rats. ***Int J Oral Maxillofac Surg.*** 42:627-631, 2013
2. Saito S, Hasegawa S, Sekita A, Bakalova R, Furukawa T, Murase K, Saga T, Aoki I: Manganese-enhanced MRI reveals early-phase radiation-induced cell alterations in vivo. ***Cancer Res.*** 73:3216-24, 2013.
3. Sawada K, Horiuchi-Hirose M, Saito S, Aoki I: MRI-based morphometric characterizations of sexual dimorphism of the cerebrum of ferrets (Mustela putorius). ***Neuroimage.*** 2013 *in press*
4. Ota S, Takahashi Y, Tomitaka A, Yamada T, Kami D, Watanabe M, Takemura Y:Transfection efficiency influenced by aggregation of DNA/polyethylenimine max/magnetic nanoparticle complexes ***J Nanoparticle Res***. 15:1-12, 2013.
5. Song Z, Yamada T, Shitara H and Takemura Y: Quantitative Analysis of Transverse Cracking of Rail using Eddy Current Non-Destructive Testing ***Appl Mechan Mat.*** 249-250:70-75, 2013.
6. 神奈川新聞　平成２５年１１月８日　「未来医療への架け橋　がん治療　磁石の力応用試みる」
7. なお、平成 25 年度においては本研究関連の特許申請(PCT)を 5 件行った。

Circulation
JOURNAL OF THE AMERICAN HEART ASSOCIATION



# Prostaglandin $E_2$ Inhibits Elastogenesis in the Ductus Arteriosus via EP4 Signaling

Utako Yokoyama, Susumu Minamisawa, Aki Shioda, Ryo Ishiwata, Mei-Hua Jin, Munetaka Masuda, Toshihide Asou, Yukihiko Sugimoto, Hiroki Aoki, Tomoyuki Nakamura and Yoshihiro Ishikawa

*Circulation.* 2014;129:487-496; originally published online October 21, 2013;
doi: 10.1161/CIRCULATIONAHA.113.004726
*Circulation* is published by the American Heart Association, 7272 Greenville Avenue, Dallas, TX 75231

Print ISSN: 0009-7322. Online ISSN: 1524-4539

# Prostaglandin $E_2$ Inhibits Elastogenesis in the Ductus Arteriosus via EP4 Signaling

Utako Yokoyama, MD, PhD; Susumu Minamisawa, MD, PhD; Aki Shioda, MS; Ryo Ishiwata, MS; Mei-Hua Jin, PhD; Munetaka Masuda, MD, PhD; Toshihide Asou, MD, PhD; Yukihiko Sugimoto, PhD; Hiroki Aoki, MD, PhD; Tomoyuki Nakamura, MD, PhD; Yoshihiro Ishikawa, MD, PhD

***Background***—Elastic fiber formation begins in mid-gestation and increases dramatically during the last trimester in the great arteries, providing elasticity and thus preventing vascular wall structure collapse. However, the ductus arteriosus (DA), a fetal bypass artery between the aorta and pulmonary artery, exhibits lower levels of elastic fiber formation, which promotes vascular collapse and subsequent closure of the DA after birth. The molecular mechanisms for this inhibited elastogenesis in the DA, which is necessary for the establishment of adult circulation, remain largely unknown.

***Methods and Results***—Stimulation of the prostaglandin $E_2$ ($PGE_2$) receptor EP4 significantly inhibited elastogenesis and decreased lysyl oxidase (LOX) protein, which catalyzes elastin cross-links in DA smooth muscle cells (SMCs), but not in aortic SMCs. Aortic SMCs expressed much less EP4 than DASMCs. Adenovirus-mediated overexpression of LOX restored the EP4-mediated inhibition of elastogenesis in DASMCs. In EP4-knockout mice, electron microscopic examination showed that the DA acquired an elastic phenotype that was similar to the neighboring aorta. More importantly, human DA and aorta tissues from 7 patients showed a negative correlation between elastic fiber formation and EP4 expression, as well as between EP4 and LOX expression. The $PGE_2$-EP4-c-Src-phospholipase C (PLC)γ–signaling pathway most likely promoted the lysosomal degradation of LOX.

***Conclusions***—Our data suggest that $PGE_2$ signaling inhibits elastogenesis in the DA, but not in the aorta, through degrading LOX protein. Elastogenesis is spatially regulated by $PGE_2$-EP4 signaling in the DA. (***Circulation.*** **2014;129:487-496.)**

**Key Words:** elasticity ■ muscle, smooth ■ pediatrics ■ prostaglandins ■ signal transduction

Elastic fibers are the largest structures in the extracellular matrix. Beginning with the onset of pulsatile blood flow in the developing aorta and pulmonary artery, smooth muscle cells (SMCs) in the vessel wall produce a complex extracellular matrix that ultimately defines the mechanical properties that are critical for proper function of the neonatal and adult vascular system.[1] As such, hemodynamics and mechanical stress are considered to be the main regulators in the formation of the vascular elastic fiber system during development.[2]

**Clinical Perspective on p 496**

The ductus arteriosus (DA) and its connecting elastic arteries (ie, the descending aorta and the main pulmonary trunk) are exposed to essentially the same mechanical forces and hemodynamics. However, since 1914, it has been widely recognized in multiple species that the DA exhibits sparse elastic fibers in the middle layer compared with adjacent elastic arteries, as well as disassembly and fragmentation of the internal elastic lamina.[3–8] In the human fetal aorta, newly synthesized uncrosslinked elastin appears at 23 weeks of gestational age to be unevenly distributed on the surface of microfibrils, where it forms continuous strips of variable width.[9] However, the DA exhibits fewer elastic fibers than the aorta.[4,6] This decreased elastogenesis is the hallmark of the vascular remodeling of the DA in humans and a variety of other species.[3–7] It has been suggested that this muscular phenotype of the DA allows it to collapse easily at birth when prostaglandin $E_2$ ($PGE_2$) is withdrawn and blood flow between the aorta and the pulmonary artery is reduced, thereby permitting immediate postnatal closure of the DA. Conversely, it is known that abnormalities of elastic fibers and elastic lamina are primarily responsible for the persistence of the DA in some human cases.[10,11] These abnormalities likely prevent intimal cushion formation and make it difficult to collapse the arterial wall. Therefore, it is

Received July 2, 2013; accepted October 7, 2013.

From the Cardiovascular Research Institute, Yokohama City University, Yokohama, Japan (U.Y., S.M., A.S., R.I., M.-H.J., Y.I.); the Department of Life Science and Medical Bioscience, Waseda University Graduate School of Advanced Science and Engineering, Tokyo, Japan (S.M., R.I.); the Department of Cell Physiology, Jikei University School of Medicine, Tokyo, Japan (S.M.); the Department of Surgery, Yokohama City University, Yokohama, Japan (M.M.); the Department of Cardiovascular Surgery, Kanagawa Children's Medical Center, Yokohama, Japan (T.A.); the Department of Pharmaceutical Biochemistry, Kumamoto University, Kumamoto, Japan (Y.S.); Cardiovascular Research Institute, Kurume University, Kurume, Japan (H.A.); and the Department of Pharmacology, Kansai Medical University, Osaka, Japan (T.N.).

**The online-only Data Supplement is available with this article at http://circ.ahajournals.org/lookup/suppl/doi:10.1161/CIRCULATIONAHA.113.004726/-/DC1.**

Correspondence to Susumu Minamisawa, MD, PhD, Department of Cell Physiology, Jikei University School of Medicine, Tokyo 105-8461, Japan. E-mail sminamis@jikei.ac.jp

important to understand the molecular mechanisms of how elastogenesis is regulated in the DA. Although Hinek et al[12,13] have demonstrated that truncated 52-kDa tropoelastin and the reduction of elastin binding protein negatively regulates elastic fiber formation in the DA, the mechanisms for impaired elastogenesis in the DA wall are not yet fully understood, despite nearly a century of research.[8]

During mid- to late gestation, fetuses are exposed to abundant $PGE_2$ that is released from the placenta[14] in accordance with the time course of impaired elastic fiber formation in the DA. The biological effects of $PGE_2$ depend on the prostanoid EP receptor subtypes EP1 through EP4[15]. Among the EP subtypes, EP4 is highly expressed in the DA of multiple species, including mice, rats, and humans, and regulates the DA muscular tone.[16–19] In addition to the DA muscular contraction, remodeling of the extracellular matrix during the fetal and neonatal period is necessary to complete the anatomical closure of the DA.[16,20,21] Our previous studies have demonstrated the role of $PGE_2$-EP4 signaling in DA remodeling, in which EP4 stimulation promotes intimal thickening, which is characteristic of the remodeling of the DA, in a hyaluronan-dependent and -independent manner.[16,21–23]

In this context, we hypothesized that $PGE_2$ inhibits elastogenesis in the DA through $PGE_2$-EP4 signaling. In the present study, we examined the molecular mechanisms of the inhibitory regulation of elastogenesis in human DA tissues and rodent DASMCs. We demonstrated that activation of EP4 promoted degradation of the mature lysyl oxidase (LOX) protein, a cross-linking enzyme for elastic fibers, only in the DA (and not in the aorta), leading to poor elastogenesis.

## Methods

Expanded methods are described in the online-only Data Supplement.

### Animals and Tissues

We used Wistar rat fetuses from timed-pregnant mothers (SLC Inc., Hamamatsu, Japan). Pooled tissues of the DA, aorta, and pulmonary arteries were obtained from rats on day 21 of gestation (n>60). Generation and phenotypes of EP4-knockout mice have been described previously.[17] All mice were C57BL/6 background littermates from heterozygote crosses. All animal studies were approved by the institutional animal care and use committees of Yokohama City University and Waseda University.

### Human Tissues of the DA

Human DA tissues were obtained from Yokohama City University Hospital and Kanagawa Children's Medical Center at the time of corrective operations. Detailed patient information is summarized in Table I in the online-only Data Supplement. The study was approved by the human subject committees at both Yokohama City University and Kanagawa Children's Medical Center. All samples were obtained after receiving written informed parental consent.

### Tissue Staining and Immunohistochemistry

Elastic fiber formation was evaluated by Elastica van Gieson staining. Immunohistochemical analysis was performed as previously described.[16] A color extraction method using BIOREVO bz-9000 and associated software (KEYENCE, Osaka, Japan) was performed to quantify elastic fiber formation and expression of EP4 and LOX. Three serial paraffin-embedded sections per each patient were subjected to elastica staining and immunohistochemistry. More than 19 fields in the smooth muscle layer of the DA and aorta were examined in each slide. The area stained dark purple indicated elastic fibers and diaminobenzidine (DAB)-stained colors, EP4- or LOX-positive areas, were extracted from matched area and counted using the software. Correlations of elastic fiber formation and EP4 and LOX expression were examined using >19 independent fields within 1 patient. We examined sections from a total of 7 patients, and the correlation coefficient and *P* value of each patient are shown in Table II in the online-only Data Supplement.

### Immunocytochemistry

Vascular SMCs were plated on glass coverslips in 10% FBS in DMEM. The culture medium was then changed to 10% FBS in DMEM/F-12 alone, $PGE_2$, AE1-329, sulprostone, butaprost, or β-aminopropionitrile fumarate (day 1). Each drug was added on day 4. To examine the effect of silencing EP4 on elastic fiber formation, reverse transfection of DASMCs with EP4-targeted siRNA was performed according to the manufacturer's instructions on days 1 and 4, and treated with AE1-329 on days 2 and 5. To examine the effect of overexpression of LOX or EP4, the cells were infected with adenoviruses at 10 multiplicities of infection on days 1 and 4. AE1-329 was added to the cells on days 2 and 5. All cells were fixed in 10% buffered formalin on day 7. The fixed cells were stained with anti-elastin antibody as previously described.[22] All images were taken using a Nikon TE2000 (Nikon Instruments Inc, Tokyo, Japan) and processed under the same settings.

### Quantitative Measurement of Insoluble Elastin

Newly synthesized insoluble elastin was measured as previously described.[24] Briefly, DASMCs were subconfluently plated on 60-mm dishes. Three days after plating, 20 μCi [$^3$H]valine was added to each dish (day 0). AE1-329 (1 μmol/L) or phosphate-buffered saline was added on days 0 and 4. The cells were harvested in 0.1 mol/L acetic acid on ice on day 7. The cells were boiled in 0.1N NaOH for 1 h. The insoluble pellets were boiled with 5.7N HCl for 1 h. The radioactivity was measured with a scintillation counter.

### Statistical Analysis

Data are shown as the mean±SEM of independent experiments. The Mann–Whitney *U* test, Kruskal-Walis test, and Pearson correlation coefficient were used to determine the statistical significance of the data. A value of $P<0.05$ was considered significant.

## Results

### EP4 Signaling Inhibits Elastogenesis in the DA In Vivo

In the late gestation period, the DA exhibits disassembly and fragmentation of the internal elastic lamina and sparse elastic fibers in the middle layer compared to its two connecting arteries, the aorta and the pulmonary artery (Figure 1A), despite the fact that they are exposed to essentially the same hemodynamics. The expression of rat EP4 is greater in the DA than in the aorta and the pulmonary artery on the 21st day of gestation (day 21; Figure 1B).[16] We examined the association between the expression of EP4 mRNA and elastogenesis in developing mouse fetuses (Figure 1C). In day 12.5 mice, organized elastic fibers were not observed in either the DA or the aorta, whereas in situ hybridization analysis revealed that the expression of EP4 mRNA was clearly higher in the DA than in the aorta or the pulmonary artery. In day 16.5 and day 18.5 mice, the formation of elastic fibers was observed more clearly in the aorta than in the DA. In these developing stages, obvious abundant expression of EP4 mRNA was observed in the DA, but not in the aorta. To examine the effect of EP4

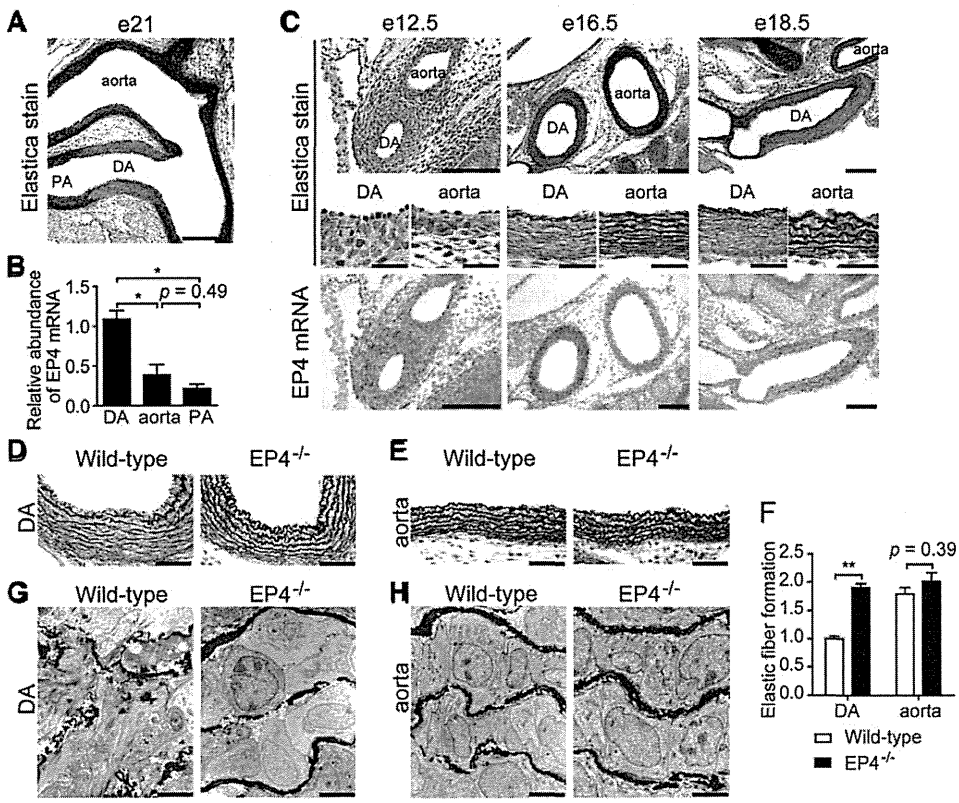


**Figure 1.** EP4 signaling attenuated elastic fiber formation in vivo. **A**, Elastica van Gieson stain (elastica stain) of rat fetus on day 21 of gestation (e21). **B**, Expression of EP4 mRNA of the rat ductus arteriosus (DA), aorta, and pulmonary artery (PA) on day 21 of gestation. n=6. **C**, Developmental changes in elastic fiber formation and EP4 mRNA by in situ hybridization in mouse fetus on days 12.5 (e12.5), 16.5 (e16.5), and 18.5 (e18.5) of gestation. Expression of EP4 mRNA was higher in the DA than in the aorta and pulmonary artery. Conversely, elastic fiber formation is sparser in the DA than in the other arteries. **D**, **E**, **G**, and **H**, Elastica stain and electron microscopic images of wild-type and EP4$^{-/-}$ mice on day 18.5 of gestation. Elastic fiber formation was restored in the DA of EP4$^{-/-}$ mice. **F**, Quantification of the elastic fiber formation of **D** and **E** using a color extraction method. n=8. *$P$<0.05, **$P$<0.01. Scale bars, 200 μm (**A**); 100 μm (**C**, **upper** and **lower**); 50 μm (**D**, **E**); 20 μm (**C**, **middle**); 5 μm (**G**, **H**).

on elastogenesis in vivo, we examined elastic fiber formation in the DA of EP4$^{-/-}$ mice. In EP4$^{-/-}$ mice, which die postnatally as a result of persistent patent DA (PDA),[17,25] we found that the DA acquired an elastic phenotype that was similar to that of the neighboring aorta, as determined by elastica staining (Figure 1D and 1E), a color extraction method of elastica staining (Figure 1F), and electron microscopic examination (Figure 1G and 1H).

## Human Vascular Tissues Show a Negative Correlation Between Elastic Fibers and EP4 Expression

We also investigated the relationship between elastic fiber formation and EP4 expression in surgical samples from 7 patients with coarctation of the aorta who underwent surgical repair of aortic narrowing (Figure 2A, Table I in the online-only Data Supplement). In concurrence with the findings in rodents, there was less elastic fiber formation in the DA than in the normal aorta, and the cells stained with anti-EP4 antibody were far more abundant in the DA (Figure 2B). Indeed, statistical analysis revealed that the correlation was significant between the amount of EP4 expression and the degree of inhibited elastic fiber formation (Figure 2C, Table II in the online-only Data Supplement). Thus, elastogenesis is inhibited when EP4 is abundant. Taken together, these in vivo data suggest that EP4 plays a primary role in the inhibition of elastogenesis of the DA in humans and rodents.

## EP4 Signaling Inhibits Elastogenesis in DASMCs

To clarify the role of EP4 in elastogenesis in detail, we evaluated the elastic fiber assemblies in rat DASMCs using an in vitro system, as reported previously.[24] In the control group, DASMCs developed an abundant meshwork of elastic fibers (Figure 3A). In the presence of PGE$_2$ or the EP4 agonist ONO-AE1-329, however, DASMCs developed a poor meshwork of elastic fibers. Neither the EP1/3 agonist sulprostone nor the EP2 agonist butaprost had any effect on elastic fiber development. LOX is a cross-linking enzyme that forms insoluble mature elastic fibers. Its specific small molecule inhibitor β-aminopropionitrile fumarate impaired elastic fiber formation (Figure 3A). To quantify the amount of mature (ie, cross-linked) elastic fibers inhibited by EP4 stimulation, we metabolically labeled newly synthesized elastin with [$^3$H]valine, and measured the incorporation of [$^3$H]valine in the NaOH-insoluble fraction of these cells, which reflects the amount of newly synthesized mature elastic fibers.[24] As shown in Figure 3B, in DASMCs, we detected a significant decrease in the incorporation of [$^3$H]-valine into the insoluble fraction when ONO-AE1-329 was added to the medium (Figure 3B). When the expression of EP4 mRNA was decreased by 89%

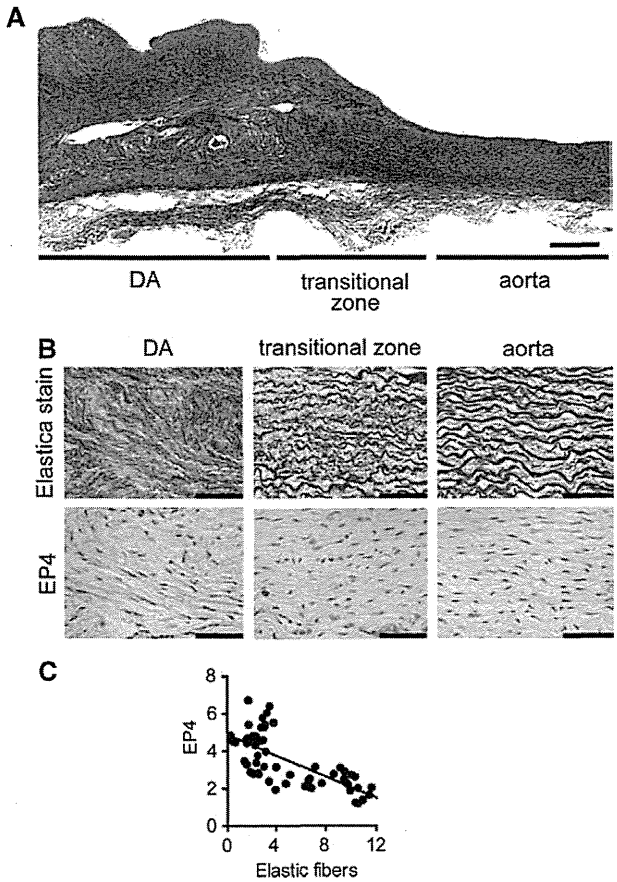


**Figure 2.** Human vascular tissues show a negative correlation between elastic fibers and EP4 expression. **A**, A representative image of the elastica stain of a human neonatal vessel. **B**, Elastica stain and immunohistochemistry for EP4 in human neonatal vessels. **C**, Representative results of quantification of elastic fiber formation and EP4 protein expression using a color extraction method. Values are shown in arbitrary units. Scale bars, 200 μm (**A**); 50 μm (**B**).

by RNA interference, DASMCs developed elastic fiber formation even in the presence of ONO-AE1-329 (Figure 3C). To further confirm the existence of EP4-mediated impaired elastic fiber formation, we used rat aortic SMCs, which express much less EP4 than DASMCs (Figure 3D). When EP4 was forcibly expressed in aortic SMCs by EP4 gene transfer, elastogenesis was markedly impaired by ONO-AE1-329, whereas ONO-AE1-329 did not attenuate elastic fiber formation in the LacZ control (Figure 3E). These in vitro results indicate that $PGE_2$-EP4 stimulation is responsible for the impaired elastogenesis of the DA.

## EP4 Signaling Inhibits Elastic Fiber Formation by Decreasing LOX Protein

In the process of elastic fiber assembly, soluble elastin precursors (tropoelastin) are deposited on microfibrils.[1,26] They are then cross-linked by LOX, which confers elastic properties to elastic fibers.[27] Inactivation of the *LOX* gene is known to cause structural alterations in the arterial walls, leading to cardiovascular abnormalities.[28] In this context, we investigated the expression of LOX protein in human surgical samples. In contrast to EP4, there were significantly fewer cells stained with anti-LOX antibody in the DA (Figure 4A). When elastic fiber formation and the expression of EP4 and LOX were quantified, LOX expression was positively correlated with elastic fiber formation, whereas it was negatively correlated with EP4 expression (Figure 4B, Table II in the online-only Data Supplement). Interestingly, elastic fiber formation and EP4- or LOX-positive cells in the transitional zone appeared intermediate between the DA and aorta. We think that this finding supports previous reports that suggested that the coarctative ridge, a narrowed pathological segment in the aorta, is formed by mixed tissues from the native aorta and migrated tissues of DA origin.[29,30]

Next, we examined the effect of EP4 stimulation on LOX protein expression. We found that the amount of mature LOX form was significantly decreased in the culture media of DASMCs and DASMC lysates in the presence of $PGE_2$ and ONO-AE1-329 (Figure 4C and 4D). The effects of ONO-AE1-329 were dose- and time-dependent (Figure 4E and 4F). Other EP isoform-specific agonists had little effect. Interestingly, stimulation of EP4 did not change the expression levels of tropoelastin and fibrillin-1 proteins, which are the main components of elastic fibers (Figure IA–ID in the online-only Data Supplement). In the next LOX detection, we used whole cell lysate containing both intracellular and extracellular LOX protein. Although these EP4-mediated effects were not detected in aortic SMCs (ASMCs), the EP4 agonist significantly decreased the expression of LOX protein in ASMCs when EP4 expression was induced using the adenovirus (Figure 4G and 4H). When LOX expression was induced using the adenovirus (Figure IIA and IIB in the online-only Data Supplement), elastogenesis was largely restored in the ONO-AE1-329–treated DASMCs (Figure 4I). Thus, the reduction in LOX played a primary role in the EP4-mediated impairment of elastogenesis. The expression levels of matrix metalloproteinases and their activity were not altered in the DASMCs by EP4 stimulation (Figure IIIA and IIIB in the online-only Data Supplement). Nor was there any difference in matrix metalloproteinase 2 activity between rat tissues of the DA and aorta (Figure IIIC in the online-only Data Supplement), suggesting that EP4 signaling plays a role in inhibiting elastogenesis, but not in promoting elastolysis in the DA.

## The c-Src-PLC Signal Pathway Plays a Role in the $PGE_2$-EP4–Induced Reduction in LOX Protein

Next, we examined the downstream signal pathway responsible for the EP4-mediated reduction in LOX protein expression levels. Although our previous studies have demonstrated that cAMP and its downstream pathways play a primary role in EP4-mediated DA remodeling,[16,22,23] the cAMP–protein kinase A or cAMP–exchange protein activated by the cAMP pathway did not play a role in the EP4-mediated reduction in LOX protein (Figure 5A and 5B). Instead, we found that the EP4-induced reduction in LOX protein was restored by the PLC inhibitor U73122 (Figure 5C–5E), but not by Gβγ, protein kinase C, or phosphoinositide 3-kinase inhibitors (gallein, bisindolylmaleimide I, LY294002; Figure 5C and 5D). Furthermore, the PLC activator *m*-3M3FBS significantly decreased the expression levels of LOX protein in DASMCs

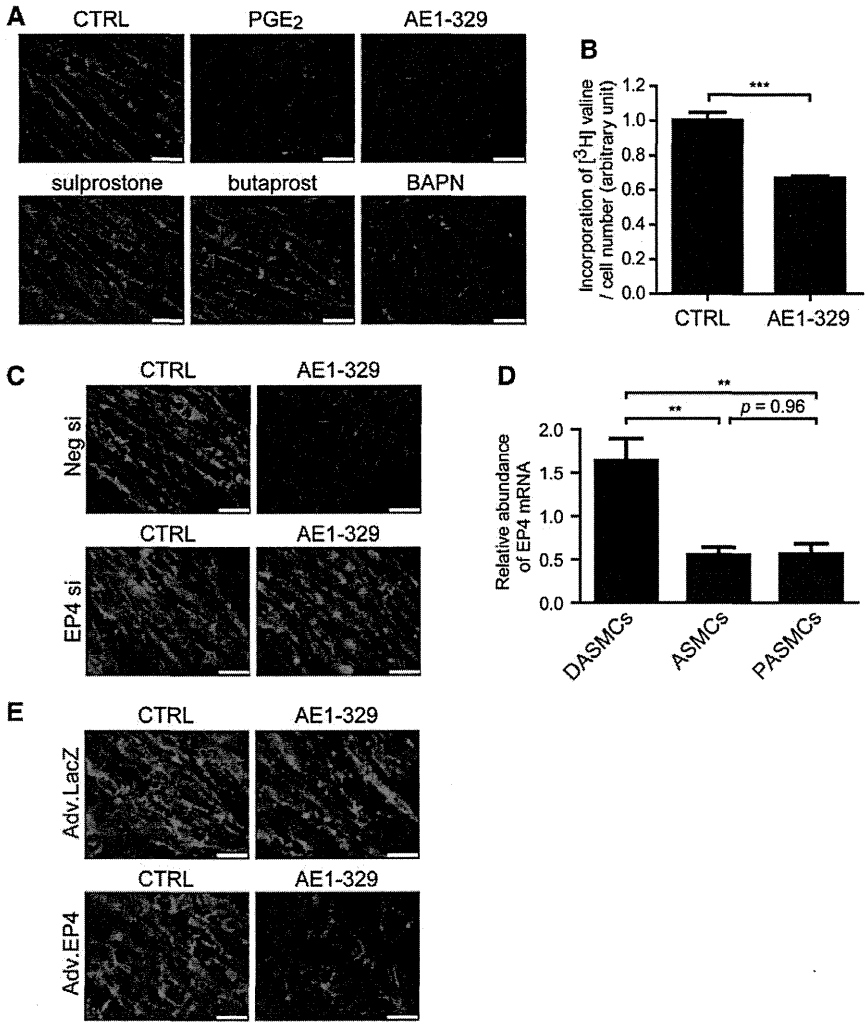


**Figure 3.** EP4 signaling attenuated elastic fiber formation in vitro. **A** and **C**, Immunostaining for elastin (red) and DNA (blue) of ductus arteriosus smooth muscle cells (DASMCs) treated with each drug indicated or EP4-targeted siRNA (EP4 si). AE1-329 indicates ONO-AE1-329; CTRL, control; and Neg si, negative control siRNA. Pharmacological activation of EP4 by ONO-AE1-329 attenuated elastic fiber formation. **B**, Incorporation of [$^3$H]valine was quantified in DASMCs treated with or without AE1-329. n=8, ***$P$<0.001. **D**, Expression of EP4 mRNA in DASMCs, aortic SMCs (ASMCs), and pulmonary SMCs (PASMCs). n=6, **$P$<0.01. **E**, Immunostaining for elastin (red) and DNA (blue) of the EP4-or LacZ-overexpressing ASMCs treated with or without AE1-329. Activation of EP4 did not affect elastic fiber formation in LacZ-overexpressing ASMCs, whereas it decreased elastic fiber formation in EP4-overexpressing ASMCs. Each drug was used at 1 μmol/L. Scale bars, 20 μm.

(Figure 5F). Because several recent studies have demonstrated that PGE$_2$ promotes cancer cell migration via the EP4–c-Src signal pathway[31,32] and that c-Src plays a critical role in the phosphorylation of PLCγ in several cell types,[33,34] we hypothesized that the c-Src-PLCγ signal pathway may be involved. We found that ONO-AE1-329 significantly increased PLCγ1 phosphorylation (Figure 5G). In contrast, the Src-family kinase inhibitor PP2 significantly decreased PLCγ1 phosphorylation (Figure 5H and 5I) and restored the reduction in LOX protein induced by ONO-AE1-329 (Figure 5J and 5K). These results support our hypothesis that the c-Src-PLCγ signal pathway plays a primary role in the PGE$_2$-EP4-induced reduction in LOX protein.

## EP4 Signaling Promotes LOX Degradation in Lysosomes

Although ONO-AE1-329 decreased the expression of LOX protein in DASMCs, we found that ONO-AE1-329 did not decrease the mRNA expression of LOX (Figure 6A). Active LOX is synthesized as a 50-kDa inactive LOX proenzyme (pro-LOX), which is secreted into the extracellular space. Pro-LOX is then processed by proteolysis into a functional 32 kDa enzyme LOX and an 18-kDa propeptide.[27,35] Using a pro-LOX–specific antibody, we found that the pro-LOX protein itself was not decreased by ONO-AE1-329 (Figure 6B and 6C), indicating that LOX was decreased post-translationally. BMP1 is a major protease that cleaves pro-LOX in the extracellular space.[27] However, ONO-AE1-329 did not change the expression of BMP1 mRNA or protein in DASMCs (Figure IVA and IVB in the online-only Data Supplement). Instead, we found that lysosomal degradation inhibitors, such as $NH_4Cl$ and bafilomycin, eliminated the EP4-induced reduction in LOX protein (Figure 6D and 6E). These lysosomal degradation inhibitors also restored the PLC-mediated reduction in LOX protein (Figure 6F and 6G). Furthermore, we found that the clathrin-mediated endocytosis inhibitors chlorpromazine and phenylarsine oxide similarly restored the EP4-induced reduction in LOX protein (Figure 6H–6J). Administration of chlorpromazine also restored the PLC-induced reduction in LOX protein (Figure 6K and 6L). In comparison, the caveolar endocytosis inhibitor methyl-beta-cyclodextrin (MβCD), the macropinocytosis inhibitor ethylisopropylamiloride (EIPA), and the proteosomal inhibitor MG132 showed little or no effect on LOX protein reduction (Figure VA–VC in the online-only Data Supplement). These data suggest that PGE$_2$-EP4-PLC stimulation promotes the degradation of the LOX protein in lysosome through clathrin-mediated endocytosis.

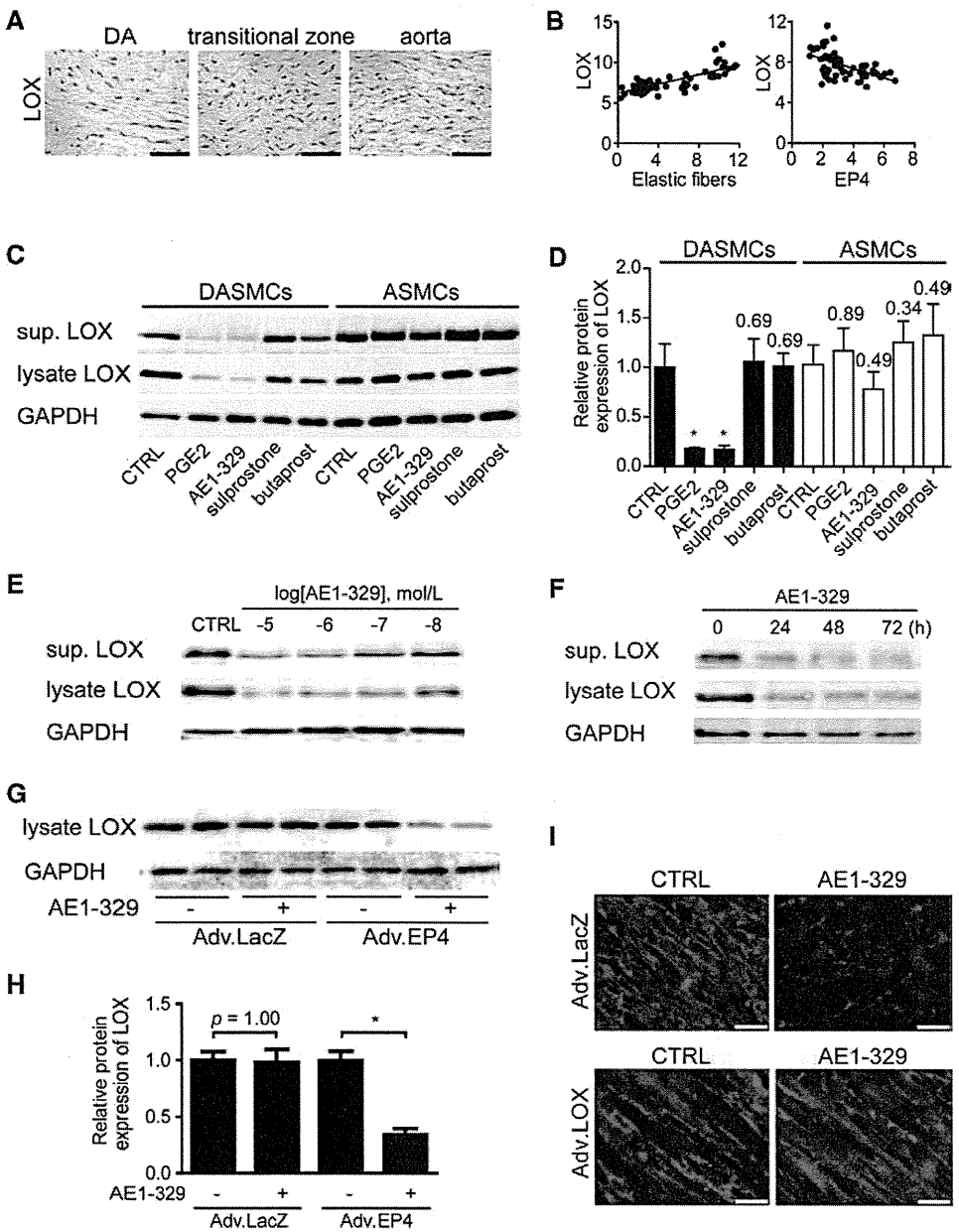


**Figure 4.** EP4 signaling attenuated elastic fiber formation via decreased lysyl oxidase (LOX) expression. **A**, Representative images of immunohistochemistry for LOX in human neonatal vessels. **B**, Representative results of quantification of elastic fiber formation, LOX, and EP4 protein expression using a color extraction method. Values are shown in arbitrary units. **C**, Western blotting for LOX in surpernatant (sup.) and lysate of smooth muscle cells (SMCs) treated for 72 h. **D**, Quantification of **C**. n=4, **P*<0.05 vs CTRL. Numbers on the bars indicate *P* values. Administration of prostaglandin $E_2$ ($PGE_2$) or the EP4 agonist AE1-329 decreased the mature LOX form in both supernatant and lysate of ductus arteriosus SMCs (DASMCs) but not in aortic SMCs (ASMCs). **E**, Dose-dependent effects of AE1-329 (24 h incubation) on LOX protein in DASMCs. **F**, Time-dependent reduction in LOX protein in DASMCs. **G**, Protein expression of LOX was decreased in EP4-overexpressing ASMCs (Adv. EP4) treated with AE-329 for 24 h. **H**, Quantification of **G**. n=4, **P*<0.05 vs CTRL. **I**, Immunostaining for elastin (red) and DNA (blue) of the LOX- or LacZ-overexpressing DASMCs treated with or without AE1-329. Each drug was used at 1 μmol/L. Scale bars, 50 μm (**A**); 20 μm (**I**).

## Discussion

Although it is widely recognized in multiple species that the DA exhibits sparse elastic fibers in the middle layer and disassembly and fragmentation of the internal elastic lamina, the molecular mechanism for these has not yet been identified. The current study demonstrated a novel role of $PGE_2$ in spatially regulating elastogenesis by LOX protein degradation via the EP4-c-Src-PLCγ signal pathway in the DA, which contributes to the transition from fetal to neonatal circulation. Previous studies have demonstrated that abnormalities of elastic fibers are primarily responsible for PDA in some human cases.[10,11] According to the Gittenberger-de Groot group's[10] observation, there are several types of abnormal elastogenesis that can cause PDA. The following 2 types are of particular importance: (1) thickened subendothelial elastic lamina with sparse or slightly increased elastic fibers in the media, and (2) aortification of the ductal wall. PDA with aortification of the ductal wall in EP4-knockout mice resembles the latter phenotype. These abnormalities of elastic fibers are likely to prohibit intimal cushion formation and make it difficult to collapse the arterial wall. This suggests that the control of elastogenesis is clinically important. Pharmacological treatment for PDA, such as indomethacin after birth, may have an adverse effect on the inhibition of elastic fiber formation in the DA, especially in premature infants. This should be further investigated in a future study.

The EP4 receptor is highly expressed in the DA compared to the adjacent arteries[16]; it is coupled to Gαs and increases intracellular cAMP formation. The roles of EP4-cAMP signaling have been well studied in the DA. We and others have demonstrated that EP4 signaling induces vasodilation and hyaluronan-mediated vascular remodeling of the DA through cAMP-dependent protein kinase A[16,21,23] and that it promotes the migration of DASMCs and subsequent intimal thickening

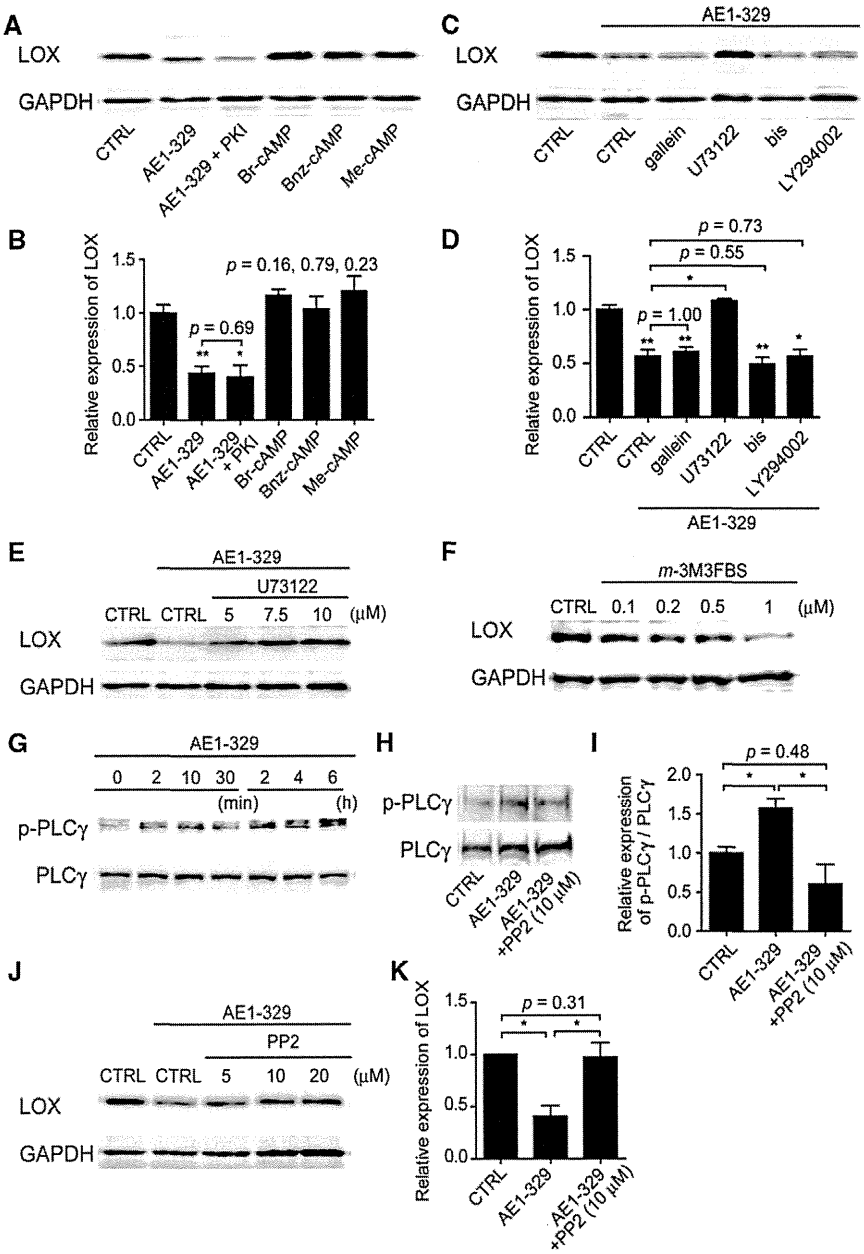


**Figure 5.** EP4 signaling decreased lysyl oxidase (LOX) protein via the c-Src-PLCγ pathway in ductus arteriosus smooth muscle cells (DASMCs). **A**, LOX protein expression in DASMCs treated with nonselective (Br-cAMP, 50 μmol/L), protein kinase A (PKA)-selective (Bnz-cAMP, 50 μmol/L) or Epac-selective (Me-cAMP, 50 μmol/L) cAMP analogs for 24 h. The AE1-329 was administered in the presence or absence of the PKA inhibitor PKI (10 μmol/L). **B**, Quantification of **A**. n=4–6, *$P$<0.05, **$P$<0.01 vs CTRL. cAMP signaling did not affect the EP4-mediated reduction of LOX protein. **C**, LOX protein expression in DASMCs treated with gallein (Gβγ inhibitor, 10 μmol/L), U73122 (PLC inhibitor, 10 μmol/L), bis (bisindolylmaleimide: PKC inhibitor, 10 μmol/L), or LY294002 (PI3K inhibitor, 1 μmol/L) in the presence of AE1-329. **D**, Quantification of **C**. n=4–6, *$P$<0.05, **$P$<0.01 vs CTRL. Inhibition of PLC eliminated the EP4-mediated reduction of LOX protein. **E**, Dose-dependent effect of U73122 in DASMCs treated with AE1-329. **F**, Dose-dependent inhibitory effect of *m*-3M3FBS on LOX protein expression. **G** and **H**, Phosphorylation of PLCγ in DASMCs treated with PP2 (Src inhibitor) or AE1-329. **I**, Quantification of **H**. n=4–6, *$P$<0.05. Inhibition of Src attenuated the EP4-mediated phosphorylation of PLCγ. **J**, PP2 attenuated the EP4-mediated reduction of LOX protein. **K**, Quantification of **J**. n=4–6. *$P$<0.05. Whole cell lysate was used for LOX detection. AE1-329 was used at 1 μmol/L.

through exchange protein activated by the cAMP.[22] Additional downstream signaling pathways of EP4 have been demonstrated in other cell types. EP4 uses Gαi and phosphoinositide 3-kinase, which are generally activated by Gβγ.[36] In addition to these well-known signaling pathways of EP4, our findings revealed c-Src-PLCγ signaling as a novel EP4 downstream pathway, as well as the inhibitory role played by EP4 signaling in elastogenesis. This EP4-signaling pathway was found to be independent of cAMP signaling, including protein kinase A and exchange protein activated by the cAMP, and Gβγ and phosphoinositide 3-kinase. Studies using colorectal and lung cancer cells have suggested that β-arrestin1 bound to EP4 activates c-Src.[31,32] In the DA, however, we did not identify an association between EP4–c-Src signaling and β-arrestin1 using β-arrestin1–targeted siRNA (data not shown). Ma et al[37] clearly demonstrated that Gαs and Gαi proteins directly stimulate the kinase activity of c-Src. Because the EP4 receptor is coupled to Gαs and Gαi, direct association between these G proteins and c-Src may activate its downstream signaling in EP4-mediated degradation of LOX protein. This possibility should be validated in a future study.

LOX is a copper-dependent amine oxidase that catalyzes the cross-linking of elastin and collagen and ensures the stability of the extracellular matrix.[38] Because LOX is the isoform responsible for 80% of the LOX activity in aortic SMCs,[39] it is essential to the maintenance of the tensile and elastic features of the vascular system.[38] LOX is synthesized as a pre-protein. After signal peptide hydrolysis, enzyme glycosylation, cooper incorporation, and lysine tyrosylquinone generation, the enzyme is released into the extracellular space. Then, BMP-1 processes LOX, yielding the mature LOX form and its propeptide.[27] The mechanisms of the transcriptional regulation of

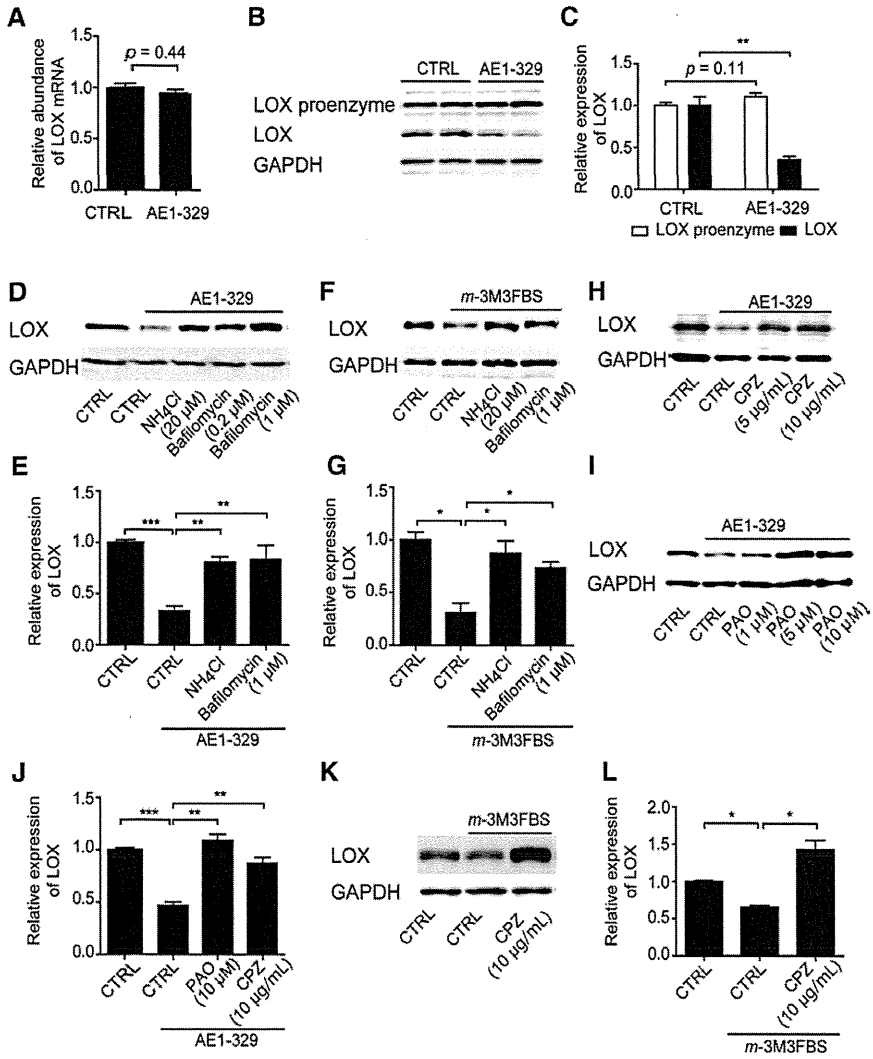


**Figure 6.** EP4 signaling decreased lysyl oxidase (LOX) protein through lysosomal degradation. **A** and **B**, Expression of LOX mRNA, pro-LOX, and LOX protein in ductus arteriosus smooth muscle cells (DASMCs) treated with AE1-329. mRNA of LOX and pro-LOX protein were not decreased by EP4 agonist in DASMCs. **C**, Quantification of **B**. n=4. **D** and **F**, Administration of lysosomal inhibitors ($NH_4Cl$ or bafilomycin) for 24 h restored the AE1-329- or *m*-3M3FBS (0.5 μmol/L)-induced reduction of LOX protein. **E** and **G**, Quantification of **D** and **F**, respectively. n=6. **H** and **I**, Administration of clathrin-mediated endocytosis inhibitors (chlorpromazine or phenylarsine oxide) for 24 h restored the AE1-329-induced reduction of LOX protein. **J**, Quantification of **H** and **I**. n=4–6. **K**, Administration of chlorpromazine for 24 h restored the *m*-3M3FBS (0.5 μmol/L) -induced reduction of LOX protein. **L**, Quantification of **K**. **P*<0.05, ***P*<0.01. ****P*<0.001. Whole cell lysate was used for LOX detection. AE1-329 was used at 1 μmol/L.

LOX have been extensively studied. Interferon-γ, transforming growth factor-β, platelet-derived growth factor, connective tissue growth factor, and angiotensin II induce LOX gene expression via the interferon regulatory factor 1 transcriptional factor in multiple tissues, including blood vessels.[40,41] On the other hand, atherogenic concentrations of low-density lipoprotein and tumor necrosis factor α reduce LOX mRNA.[42,43] Song et al[44] have also shown that interferon-γ inhibits LOX gene expression through binding to the antagonistic transcriptional factor, interferon regulatory factor 2, in vascular SMCs.

In contrast to our understanding of these transcriptional regulations of LOX, little is known regarding LOX protein metabolism. In the present study, we demonstrated for the first time that the $PGE_2$-EP4 signal promoted lysosomal degradation of LOX protein. Recently, 1 study that used lysosomal inhibitors and Vps18-deficient mice demonstrated that LOX protein was degraded through lysosomes in Purkinje cells.[45] However, the detailed molecular mechanisms triggering the degradation of LOX protein have not been reported and should be examined in future studies. Once LOX is cleaved from the proenzyme, it acts as a highly reactive enzyme. The mature LOX form catalyzes an oxidative deamination of lysine and hydroxylysine residues to peptidyl α-aminoadipic-δ-semialdehydes. These highly reactive semialdehydes can spontaneously condense to form intra- and intermolecular covalent cross-linkages.[27] Elastic fiber formation must be highly regulated to ensure the integrity of vascular and other tissues. Therefore, in addition to transcriptional regulation, the existence of protein regulation of LOX that we demonstrated in this study is physiologically reasonable.

The Rabinovitch group has extensively studied the molecular mechanisms of the sparse elastic fiber formation in the medial layer of the DA. Their studies have demonstrated that LOX activity does not differ between the lamb DA, aorta, and pulmonary artery.[46] Our study demonstrated that LOX protein was dramatically decreased by EP4 signaling in rodents and humans, suggesting that LOX activity is decreased in these DAs. Currently, we do not have a clear explanation for the apparent inconsistency in terms of LOX expression and activity. Further research is required to determine the species difference in LOX protein metabolism and activity. The Rabinovitch group also demonstrated that there is decreased insolubilization of elastin in the DA that is associated with the truncated 52-kDa tropoelastin that lacks the C terminus,[12] which is unrelated to heightened elastolytic activity.[46] Similarly, our results showed that matrix metalloproteinase 2

activity does not differ between the DA and the aorta, suggesting that impaired elastogenesis rather than enhanced elastolytic activity provides a muscular arterial property to the DA.

The present study demonstrated that LOX expression is important during development. However, LOX expression is known to be markedly responsive to a variety of pathological states, including wound repair, aging, and tumorigenesis.[41] In particular, strong evidence exists regarding the involvement of a reduction in LOX activity in the pathogenesis of vascular diseases characterized by destructive remodeling of the arterial wall. Previous reports demonstrated that aortic aneurysm and coronary dissections were related to a disturbance in LOX expression in animal models and humans.[47,48] Therefore, the regulation of LOX expression is considered an attractive therapeutic target. In this study, it should be noted that there seems to be a threshold value for EP4 expression to induce a decrease in elastic fibers and LOX (Figures 2C and 4B). In our previous report, analyses of human aortic aneurysmal tissues demonstrated that EP4 expression is greater in aneurysmal legions than that in nondiseased areas.[49] Further studies are required to investigate whether EP4-mediated LOX regulation plays a role in pathological conditions.

Taken together, these findings suggest that PGE$_2$-EP4 signaling inhibits elastogenesis in the DA by degrading LOX protein. The PGE$_2$-EP4-mediated LOX protein regulation via a previously unrecognized signaling pathway may also provide the basis for therapeutic strategies that target vascular elastogeneis.

## Acknowledgments

We thank Professor S. Narumiya (Department of Pharmacology, Kyoto University Faculty of Medicine, Kyoto, Japan) for kindly providing EP4$^{-/-}$ mice. We thank Professor S. Morita and Dr M. Taguri (Department of Biostatistics and Epidemiology, Yokohama City University, Yokohama, Japan) for assistance with statistical analysis. The adenoviruses of EP4 and LOX were kindly provided from Dr Y. Kobayashi (Matsumoto Dental University, Matsumoto, Japan) and Dr K. Yoshimura (Yamaguchi University, Yamaguchi, Japan), respectively. We also thank Yuka Sawada for histological analyses.

## Sources of Funding

This work was supported by grants from the Ministry of Health, Labor, and Welfare of Japan (Y.I.), the Ministry of Education, Culture, Sports, Science, and Technology of Japan (Y.I., U.Y., S.S., M.M., S.M.), a Grant-in-Aid for Scientific Research on Innovative Areas (23116514 and 25116719 to U.Y., 22136009 to Y.I.), the Kitsuen Kagaku Research Foundation (Y.I.), the Foundation for Growth Science (S.M.), the Yokohama Foundation for Advanced Medical Science (U.Y., S.M.), the "High-Tech Research Center" Project for Private Universities: MEXT (S.M.), MEXT-Supported Program for the Strategic Research Foundation at Private Universities (S.M.), the Vehicle Racing Commemorative Foundation (U.Y., S.M.), Miyata Cardiology Research Promotion Funds (U.Y., S.M.), the Takeda Science Foundation (Y.I., U.Y., S.M.), the Japan Heart Foundation Research Grant (U.Y.), the Kowa Life Science Foundation (U.Y.), the Sumitomo Foundation (U.Y), and the Shimabara Science Promotion Foundation (S.M.).

## Disclosures

None.

## References

1. Wagenseil JE, Mecham RP. Vascular extracellular matrix and arterial mechanics. *Physiol Rev*. 2009;89:957–989.
2. Wagenseil JE, Ciliberto CH, Knutsen RH, Levy MA, Kovacs A, Mecham RP. The importance of elastin to aortic development in mice. *Am J Physiol Heart Circ Physiol*. 2010;299:H257–H264.
3. Jager BV, Wollenman OJ. An Anatomical Study of the Closure of the Ductus Arteriosus. *Am J Pathol*. 1942;18:595–613.
4. de Reeder EG, van Munsteren CJ, Poelmann RE, Patterson DF, Gittenberger-de Groot AC. Changes in distribution of elastin and elastin receptor during intimal cushion formation in the ductus arteriosus. *Anat Embryol (Berl)*. 1990;182:473–480.
5. Ho SY, Anderson RH. Anatomical closure of the ductus arteriosus: a study in 35 specimens. *J Anat*. 1979;128(pt 4):829–836.
6. Toda T, Tsuda N, Takagi T, Nishimori I, Leszczynski D, Kummerow F. Ultrastructure of developing human ductus arteriosus. *J Anat*. 1980;131(pt 1):25–37.
7. Tada T, Kishimoto H. Ultrastructural and histological studies on closure of the mouse ductus arteriosus. *Acta Anat (Basel)*. 1990;139:326–334.
8. Schaeffer JP. The behavior of elastic tissue in the postfetal occlusion and obliteration of the ductus arteriosus (BOTALLI) in SUS SCROFA. *J Exp Med*. 1914;19:129–142.
9. Jaques A, Serafini-Fracassini A. Morphogenesis of the elastic fiber: an immunoelectronmicroscopy investigation. *J Ultrastruct Res*. 1985; 92:201–210.
10. Gittenberger-de Groot AC. Persistent ductus arteriosus: most probably a primary congenital malformation. *Br Heart J*. 1977;39:610–618.
11. Gittenberger-de Groot AC, Moulaert AJ, Hitchcock JF. Histology of the persistent ductus arteriosus in cases of congenital rubella. *Circulation*. 1980;62:183–186.
12. Hinek A, Rabinovitch M. The ductus arteriosus migratory smooth muscle cell phenotype processes tropoelastin to a 52-kDa product associated with impaired assembly of elastic laminae. *J Biol Chem*. 1993;268:1405–1413.
13. Hinek A, Mecham RP, Keeley F, Rabinovitch M. Impaired elastin fiber assembly related to reduced 67-kD elastin-binding protein in fetal lamb ductus arteriosus and in cultured aortic smooth muscle cells treated with chondroitin sulfate. *J Clin Invest*. 1991;88:2083–2094.
14. Mitchell MD, Lucas A, Etches PC, Brunt JD, Turnbull AC. Plasma prostaglandin levels during early neonatal life following term and pre-term delivery. *Prostaglandins*. 1978;16:319–326.
15. Woodward DF, Jones RL, Narumiya S. International Union of Basic and Clinical Pharmacology. LXXXIII: classification of prostanoid receptors, updating 15 years of progress. *Pharmacol Rev*. 2011;63:471–538.
16. Yokoyama U, Minamisawa S, Quan H, Ghatak S, Akaike T, Segi-Nishida E, Iwasaki S, Iwamoto M, Misra S, Tamura K, Hori H, Yokota S, Toole BP, Sugimoto Y, Ishikawa Y. Chronic activation of the prostaglandin receptor EP4 promotes hyaluronan-mediated neointimal formation in the ductus arteriosus. *J Clin Invest*. 2006;116:3026–3034.
17. Segi E, Sugimoto Y, Yamasaki A, Aze Y, Oida H, Nishimura T, Murata T, Matsuoka T, Ushikubi F, Hirose M, Tanaka T, Yoshida N, Narumiya S, Ichikawa A. Patent ductus arteriosus and neonatal death in prostaglandin receptor EP4-deficient mice. *Biochem Biophys Res Commun*. 1998;246:7–12.
18. Smith GC, Wu WX, Nijland MJ, Koenen SV, Nathanielsz PW. Effect of gestational age, corticosteroids, and birth on expression of prostanoid EP receptor genes in lamb and baboon ductus arteriosus. *J Cardiovasc Pharmacol*. 2001;37:697–704.
19. Leonhardt A, Glaser A, Wegmann M, Schranz D, Seyberth H, Nüsing R. Expression of prostanoid receptors in human ductus arteriosus. *Br J Pharmacol*. 2003;138:655–659.
20. Rabinovitch M. Cell-extracellular matrix interactions in the ductus arteriosus and perinatal pulmonary circulation. *Semin Perinatol*. 1996;20:531–541.
21. Yokoyama U, Minamisawa S, Ishikawa Y. Regulation of vascular tone and remodeling of the ductus arteriosus. *J Smooth Muscle Res*. 2010;46:77–87.
22. Yokoyama U, Minamisawa S, Quan H, Akaike T, Suzuki S, Jin M, Jiao Q, Watanabe M, Otsu K, Iwasaki S, Nishimaki S, Sato M, Ishikawa Y. Prostaglandin E2-activated Epac promotes neointimal formation of the rat ductus arteriosus by a process distinct from that of cAMP-dependent protein kinase A. *J Biol Chem*. 2008;283:28702–28709.
23. Yokoyama U, Minamisawa S, Katayama A, Tang T, Suzuki S, Iwatsubo K, Iwasaki S, Kurotani R, Okumura S, Sato M, Yokota S, Hammond HK, Ishikawa Y. Differential regulation of vascular tone and remodeling via stimulation of type 2 and type 6 adenylyl cyclases in the ductus arteriosus. *Circ Res*. 2010;106:1882–1892.
24. Hirai M, Ohbayashi T, Horiguchi M, Okawa K, Hagiwara A, Chien KR, Kita T, Nakamura T. Fibulin-5/DANCE has an elastogenic organizer activity that is abrogated by proteolytic cleavage in vivo. *J Cell Biol*. 2007;176:1061–1071.